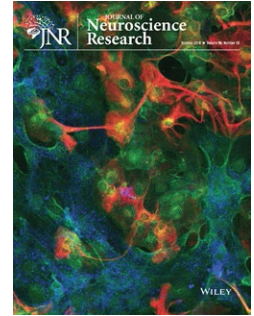




**TECHNICAL REPORT**

# Development of barium-based low viscosity contrast agents for micro CT vascular casting: Application to 3D visualization of the adult mouse cerebrovasculature

Sung-Ha Hong<sup>1</sup> | Alexander M. Herman<sup>2,3</sup> | Jessica M. Stephenson<sup>1</sup> | Ting Wu<sup>1</sup> |  
 Ali N. Bahadur<sup>4</sup> | Alan R. Burns<sup>5</sup> | Sean P. Marrelli<sup>1</sup>  | Joshua D. Wythe<sup>2,3</sup> 

<sup>1</sup>Department of Neurology, McGovern Medical School at UT Health, Houston, TX, USA

<sup>2</sup>Cardiovascular Research Institute, Baylor College of Medicine, Houston, TX, USA

<sup>3</sup>Department of Molecular Physiology and Biophysics, Baylor College of Medicine, Houston, TX, USA

<sup>4</sup>Bruker BioSpin Corporation, Billerica, MA, USA

<sup>5</sup>College of Optometry, University of Houston, Houston, TX, USA

**Correspondence**

Sean P. Marrelli, Department of Neurology, McGovern Medical School, 6431 Fannin Street, Houston, TX 77030, USA.  
 Email: Sean.P.Marrelli@uth.tmc.edu

Joshua D. Wythe, CVRI, Department of Molecular Physiology and Biophysics, Baylor College of Medicine, One Baylor Plaza, Houston, TX 77030, USA.  
 Email: wythe@bcm.edu

**Funding information**

S-H.H. was supported by an American Heart Association Postdoctoral Award (19POST34380074). A.M.H. was supported by the National Institutes of Health (5T32HL007676-27, 5T32HL007676-28) and American Heart Association Postdoctoral Award (19POST34430008). A.R.B. is supported by National Eye Institute P30 EY007551. S.P.M. is supported by the National Institute of Neurological Disorders and Stroke (R01 NS094280 and R01 NS096186) and Ignite Grant from the Huffington Foundation. J.D.W.

**Abstract**

Recent advances in three-dimensional (3D) fluorescence microscopy offer the ability to image the entire vascular network in entire organs, or even whole animals. However, these imaging modalities rely on either endogenous fluorescent reporters or involved immunohistochemistry protocols, as well as optical clearing of the tissue and refractive index matching. Conversely, X-ray-based 3D imaging modalities, such as micro CT, can image non-transparent samples, at high resolution, without requiring complicated or expensive immunolabeling and clearing protocols, or fluorescent reporters. Here, we compared two “homemade” barium-based contrast agents to the field standard, lead-containing Microfil, for micro-computed tomography (micro CT) imaging of the adult mouse cerebrovasculature. The perfusion pressure required for uniform vessel filling was significantly lower with the barium-based contrast agents compared to the polymer-based Microfil. Accordingly, the barium agents showed no evidence of vascular distension or rupture, common problems associated with Microfil. Compellingly, perfusion of an aqueous BaCl<sub>2</sub>/gelatin mixture yielded equal or superior visualization of the cerebrovasculature by micro CT compared to Microfil. However, phosphate-containing buffers and fixatives were incompatible with BaCl<sub>2</sub> due to the formation of unwanted precipitates. X-ray attenuation of the vessels also decreased overtime, as the BaCl<sub>2</sub> appeared to gradually diffuse into surrounding tissues. A second, unique formulation composed of BaSO<sub>4</sub> microparticles, generated in-house by mixing BaCl<sub>2</sub> and MgSO<sub>4</sub>, suffered none of these drawbacks. These microparticles, however, were unable to pass small diameter capillary vessels, conveniently labeling only the arterial cerebrovasculature. In summary, we present an affordable, robust, low pressure, non-toxic, and straightforward methodology for 3D visualization of the cerebrovasculature.

is supported by institutional startup funds from the Cardiovascular Research Institute at Baylor College of Medicine, the Caroline Wiess Law Fund for Research in Molecular Medicine, the Curtis and Doris K. Hankamer Foundation Basic Research Fund, and the ARCO Foundation Young Teacher-Investigator Award. Work within the Wythe lab is supported by the American Heart Association (16GRNT31330023) and the Department of Defense (W81XWH-18-1-0350).

**KEYWORDS**

brain, cerebral, micro CT, stroke, vasculature

## 1 | INTRODUCTION

Vascular casting can be used for three-dimensional (3D) analyses of large arteries and veins as well as the microvasculature (Ehling et al., 2014; Jorgensen, Demirkaya, & Ritman, 1998; Marxen et al., 2004; Vandeghinste et al., 2011). The procedure consists of injecting a pigmented or radiopaque casting material into the vasculature (such as by transcardiac perfusion) which then allows one to easily visualize the entire vasculature network in situ. Two commonly used commercial products are Microfil (Flow Tech, Inc.) and Batson's #17 compound (Polysciences, Inc). Both systems consist of monomer solutions which are mixed with a catalyst just before use to initiate subsequent polymerization following vascular perfusion. After polymerization is complete (curing), the organic portion of the sample can be chemically dissolved or optically cleared to allow for direct visualization of the perfused vascular network by stereomicroscopy without interference from surrounding tissues. If the radiopaque versions of these filling compounds are used, the intact tissue can be imaged by micro-computed tomography (micro CT). Micro CT relies on the use of X-rays, as they pass readily through biological material (unlike photons in the visual spectrum), which is why optically non-transparent samples can be imaged using this modality. In a manner analogous to a CT scan, multiple images are acquired at different angles by rotating the sample during image acquisition and back calculating the tissue's differential absorption of X-rays to generate a 3D reconstruction for volumetric rendering and quantitative analysis (Clark & Badea, 2014).

Although the above polymer-based filling solutions are excellent for many downstream uses, there are several characteristics that can limit their suitability for other end-use applications. First, due to the higher viscosity and non-miscible nature of these compounds, suprathreshold filling pressures are generally required to achieve uniform vascular filling. As a result, infusion can often induce vascular bulging or even rupture (Vasquez et al., 2011). If casting is being used to screen for pre-existing vascular deformations, a high-pressure infusion protocol would be non-optimal, as the elevated pressure may cause fragile vessels to rupture as a result of the procedure. Second, filling with these compounds cannot be reliably restricted to the arterial or venous circulations. To ensure uniform filling of the microvasculature (especially in smaller species), the procedure for preparing these polymer-based systems must be modified to lower the viscosity of the infused mixture (Ghanavati, Yu, Lerch, & Sled,

### Significance

Two-dimensional image acquisition remains the most common approach for studying and representing three-dimensional (3D) vascular preparations, despite the advent of numerous new 3D imaging modalities. One such platform, micro-computed tomography (micro CT), can rapidly generate high-resolution vascular casts following infusion of radiopaque materials without the need for tissue clearing or immunohistochemistry. Here we identify two unique barium-based contrast formulations for micro CT that can be easily prepared in the laboratory. These "homemade" formulations offer several distinctions and advantages compared to the lead-based field standard (Microfil), and enable robust and consistent 3D reconstructions of the murine cerebral vasculature using micro CT.

2014; Vasquez et al., 2011). As a result, transcardiac infusion results in continuous filling of the arterial and venous vasculatures. If a combined representation of the arterial and venous vasculature is desired, this outcome is ideal. However, if one is primarily interested in the arterial vasculature, the additional filling of the venous vasculature represents an unwanted increase in complexity for quantitative analyses and downstream interpretation.

In the following study, we sought to evaluate new radiopaque casting methods that (a) require low (physiologic) infusion pressure and (b) can be restricted to the arterial vasculature. We present a comparison of two barium-based casting formulations with the current "gold standard," Microfil MV-122 compound, for use in micro CT-based vascular imaging. Furthermore, we describe a method for preventing the image distortion that results from tissue deformation during the long acquisition times required for high-resolution micro CT imaging.

## 2 | MATERIALS AND METHODS

### 2.1 | Animals

All experimental procedures were approved by the Institutional Animal Care and Use Committees at the McGovern Medical School at UTHealth and at Baylor College of Medicine. Twenty male

C57BL6/N mice, aged 2–6 months, were used in pilot studies to establish a final procedure for aortic retrograde and transcardiac perfusion. Once the ideal parameters had been established, a total of 24 additional male C57BL6/N mice (Charles River) of 9–11 months of age were used for the imaging experiments and to generate all of the figures within this manuscript. The reason for selecting the C57BL6/N strain and only males was purely practical—we had a complete cohort of mature male mice available to complete the study. As the primary goal of the study was to develop novel contrast agents for visualizing the cerebral small vasculature via micro CT-based imaging, the first step was to characterize the different methods using as consistent a cohort and mouse preparation as possible in order to avoid any technical or biological variation. If there were a sex-based difference in the anatomical structure of the cerebral small vasculature, this variability would have confounded our initial studies, thus we confined our experiments to a single sex.

## 2.2 | Preparation of BaSO<sub>4</sub> microparticle by replacement reaction

To generate a consistent microparticle preparation of BaSO<sub>4</sub>, we produced BaSO<sub>4</sub> in the laboratory by a replacement reaction between BaCl<sub>2</sub> and MgSO<sub>4</sub>. For this reaction, we setup a syringe pump to slowly deliver BaCl<sub>2</sub> (0.25 M in dH<sub>2</sub>O) at 0.3 ml/min through polyethylene 50 (PE-50) tubing (see Figure S1 and Movie S1). The tubing was immersed in a 250 ml beaker containing 200 ml of MgSO<sub>4</sub> (0.25 M in dH<sub>2</sub>O) with rapid stirring. Three milliliters of BaCl<sub>2</sub> was delivered over 10 min, producing a fine suspension of insoluble BaSO<sub>4</sub> that immediately dispersed throughout the solution. The suspension was spun down at 300× g for 10 min. The supernatant was poured off and the BaSO<sub>4</sub> precipitate was re-suspended in saline (0.9% NaCl). The microparticles were washed two more times with saline, and then filtered through a 40 micron basket filter (Fisher Scientific, 22-363-547). The final working suspension was adjusted to 1%–2% BaSO<sub>4</sub> wt/vol in saline.

## 2.3 | Preparation of phantoms for X-ray attenuation comparison

Phantoms were generated in PE-50 tubing for Microfil MV122 (Flow Tech Inc., Carver, MA), a suspension of BaSO<sub>4</sub> prepared from commercially obtained BaSO<sub>4</sub> (Sigma-Aldrich), a suspension of BaSO<sub>4</sub> microparticles, and BaCl<sub>2</sub> (10% and 35%) in 10% unflavored gelatin (Knox, E.D. Smith Foods). For comparison, phantoms were also generated for air and saline. The working Microfil solution was prepared by mixing 5 parts of Microfil MV-122, 4 parts diluent, and 0.5 parts catalyst; these proportions are purported by the manufacturer to produce a lower viscosity solution. The phantoms were imaged as a single group by micro CT (SkyScan 1272, Bruker, MA). The X-ray attenuation of contrast agents was compared by measuring mean image intensity of the samples. Image intensities were inverted so that increased attenuation was reflected in the positive direction (Image J).

## 2.4 | Analysis of BaSO<sub>4</sub> microparticles by light microscopy and scanning electron microscopy (SEM)

For light microscopy, a droplet of BaSO<sub>4</sub> microparticles in saline was applied to a glass slide and then coverslipped. The preparation was then imaged by phase contrast (10X/0.30 PH1 objective) on a Leica DMI8 inverted microscope. For SEM analysis, a droplet of BaSO<sub>4</sub> microparticles suspended in dH<sub>2</sub>O was placed on a double-stick carbon tab affixed to a specimen holder and allowed to air dry. The dried preparation was then imaged without further processing in a Tescan Mira 3 SEM using secondary electron detection with the microscope operating at 25 keV. Images were collected from multiple locations across the sample and analyzed in ImageJ to estimate median particle size. For non-symmetric particles, the longest dimension was used to estimate particle size.

## 2.5 | Preparation of BaCl<sub>2</sub>/gelatin solutions

Gelatin solutions were prepared by adding 0, 10, or 35% of BaCl<sub>2</sub> with 2 or 10% gelatin in dH<sub>2</sub>O and heating in a water bath. The resulting gelatin solutions were added to a 1 ml glass vial and allowed to set for 2 hr at 4°C. To demonstrate whether the gelatin had hardened, a 0.35 g steel ball (steel BB) was placed on the top of the mixture and photographed.

## 2.6 | Precipitation test of BaCl<sub>2</sub> with perfusion reagents

To determine the potential of BaCl<sub>2</sub> to precipitate with different reagents used in the mouse perfusion procedure, we added 50 µl of BaCl<sub>2</sub> (1 M) to 700 µl of either dH<sub>2</sub>O, saline, PBS, phosphate-free formalin, 10% phosphate-buffered formalin, MgSO<sub>4</sub> (1 M). The phosphate-free formalin used was Shandon Formal-Fixx (Thermo Fisher) and the buffered formalin was 10% buffered formalin phosphate (Thermo Fisher). Images were taken immediately after addition of the BaCl<sub>2</sub> solution.

## 2.7 | Preparation for contrast agent infusion

Animals were injected intraperitoneally with heparin (100 U/ml, 0.2 ml per mouse; #949516, McKesson) and the anticoagulant was allowed to circulate for 5 min. Mice were then deeply anesthetized with 5% isoflurane delivered in 30% oxygen and balance nitrous oxide and then pinned to a cork surgical board. To ensure the mice did not awaken during the procedure, a 15 ml Falcon tube containing an isoflurane-wetted cotton ball was placed over their snout. The chest cavity was then opened and perfusion was performed by either of the methods described below.

Once the animal was setup for aortic or transcardiac perfusion, a syringe pump (NE-300, New Era Pump Systems, NY) was used to deliver 20 ml of room temperature PBS containing 2 mM sodium nitroprusside (2 mM; Fluka) and papaverine (150 µM; Sigma-Aldrich) to ensure all vessels were dilated and accessible to the filling

solutions. The perfusion rate was incrementally increased from 1 to 5 ml/min. Perfusion was then continued with 20 ml of room temperature 10% Formalin (Formal-Fixx, Shandon) at 5 ml/min. Pilot studies were performed with an in-line pressure transducer (Living Systems Instrumentation, VT) to ensure that the maximum infusion rate did not result in perfusion pressures exceeding 90 mm Hg. After fixation, perfusion of Microfil or barium-based contrast agents was performed by hand (see below).

### 2.7.1 | Aortic perfusion

For the retrograde perfusion via the aorta ("aortic perfusion"), a heat-tapered PE-50 tube was introduced into the abdominal aorta and advanced anteriorly (toward the heart) to a point just beneath the descending portion of the aortic arch (see Figure S2). The tubing was secured in the aorta by a suture and then further secured to the body cavity ("strain relief") by cyanoacrylate glue. The inferior vena cava was severed immediately before the start of perfusion to provide venous outflow.

### 2.7.2 | Transcardiac perfusion

Transcardiac perfusion was performed by inserting a 27G needle into the left ventricle. The needle was connected to the syringe by a short length of tubing (S-50-HL, Tygon) and plastic tubing adaptors (Cole-Parmer). The needle was secured at the apex of the heart by the application of cyanoacrylate glue at the puncture site. The tubing was glued to the body cavity for strain relief as above. The descending aorta was clamped with a hemostat to improve perfusion to the brain. The inferior vena cava was severed just prior to the start of perfusion.

### 2.7.3 | Perfusion of BaSO<sub>4</sub> microparticles

Following the fixative infusion step, a 5 or 10 ml volume of 1%–2% (wt/vol) microparticles was delivered by gentle continuous depression of the plunger. Note that the syringe had to be continually rotated and tilted during this process to prevent the microparticles from settling to the bottom of the syringe. Little resistance to infusion was felt, even toward the end of the procedure. Clear effluent from the inferior vena cava was noted throughout. Following microparticle perfusion, the brain was immediately removed and placed in a 20 ml scintillation vial containing 15 ml of 10% Formalin (Formal-Fixx, Shandon) and stored at 4°C.

### 2.7.4 | Perfusion of Microfil

Following the fixative infusion step, freshly prepared Microfil (as described for phantoms) was back-loaded into a 10 ml syringe and perfused by hand until high backpressure was felt. This high resistance to further filling was generally encountered after infusing approximately 3 ml of compound. At the end of Microfil infusion, the vena cava was sealed by electrocoagulation and the entire preparation

(intact mouse and infusion cannula with syringe) was placed on ice overnight to allow for complete curing of the polymer. The next day, the brain was removed, rinsed in PBS, then placed in 10% Formalin (Formal-Fixx, Shandon), and stored at 4°C.

## 2.8 | Stereomicroscopic imaging of infused brains

To evaluate the uniformity of contrast agent filling, isolated fixed brains were imaged using a stereomicroscope (Leica M205 FA & DFC9000 GT camera). Z-stacks of the dorsal and ventral views were captured and processed with the extended depth of field (EDOF) algorithm in LAS X (Leica).

## 2.9 | Middle cerebral artery (MCA) stroke model

The right MCA was occluded by placement of a silicone-coated filament (5–6 mm coated length, Docol) as we have described previously (Fasipe et al., 2018), but with the following modifications. Following occluder placement, the right common carotid artery and internal carotid artery were secured with sutures. At 60 min of MCA occlusion, BaSO<sub>4</sub> microparticles or Microfil was infused by the aortic perfusion method as described above. Brain removal was performed carefully to ensure the end of the occluder remained in position within the circle of Willis (CoW). Brains were then stored in fixative until imaging as described above.

## 2.10 | Ex vivo micro CT imaging

Micro CT images of the brains were obtained using a SkyScan 1272 (in the Optical and Intravital Microscopy core at BCM) or with a SkyScan 1276 (at Bruker Biospin, Billerica, MA). The brains scanned at BCM (Figures 5–7) were wrapped in Saran Wrap to reduce sample dehydration and placed in a modified Styrofoam holder for imaging. Scans were performed with the following parameters: source voltage and current (60 kV and 166  $\mu$ A), imaging voxel size was 6.6 to 6.8  $\mu$ m with 0.25  $\mu$ m Al filter. The distance of X-ray to object was set to 199.98 mm. The brains scanned at Bruker BioSpin (Figure 8) were prepared by embedding the isolated brains in low melt agarose (1%) in dH<sub>2</sub>O in a 5 ml plastic vial (ST-5MI, Axygen Scientific) as an alternative method to reduce tissue dehydration during acquisition. This alternative approach was adopted to reduce imaging artifact due to the slight sample dehydration that occurred with Saran Wrap samples. The following scan parameters were used: source and current (55 kV and 200  $\mu$ A), imaging voxel size was 6.8  $\mu$ m with 0.25  $\mu$ m Al filter. The distance of X-ray to object was set to 157.29 mm. Acquired images were reconstructed by NRecon Reconstruction software (Bruker MicroCT, Kontich, Belgium) and then rendered into 3D images in CTvox volume rendering software (Bruker MicroCT, Kontich, Belgium).

## 2.11 | Brain optical clearing and imaging

At the conclusion of micro CT scanning, brains were sectioned at 1 mm thickness and optically cleared for stereomicroscopic examination.

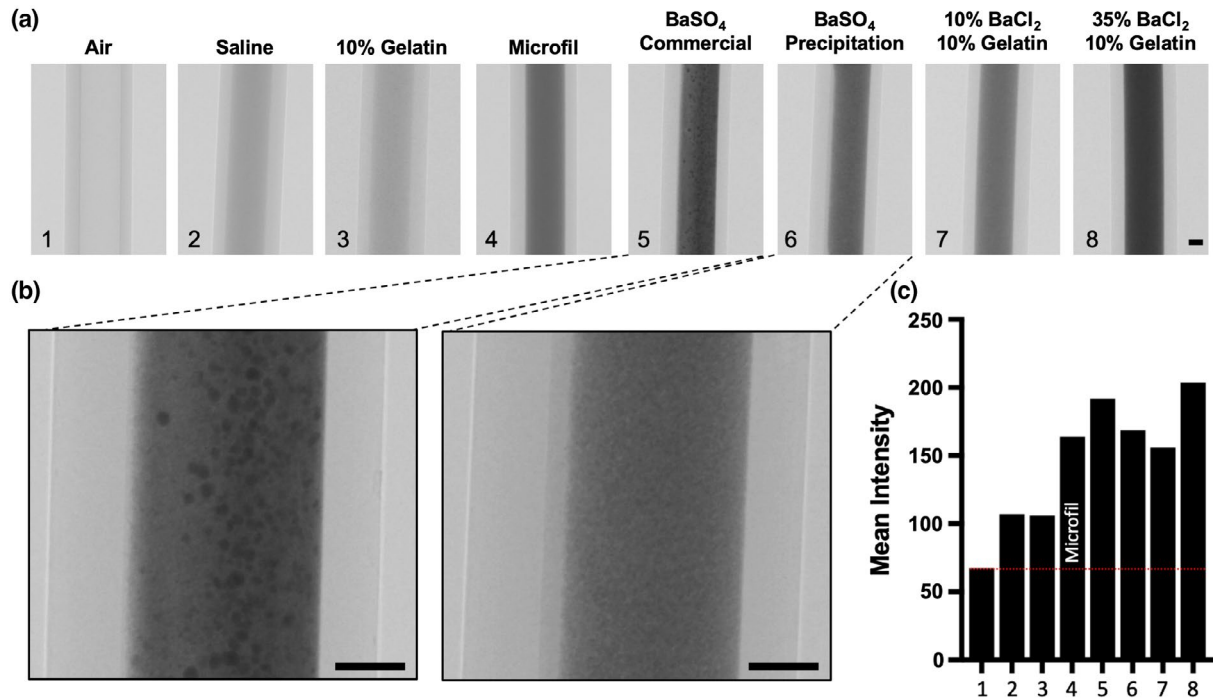


**FIGURE 1** Survey of alternative vascular casting compounds for visualizing the cerebral vasculature by micro CT. (a) Polyethylene tubes of 0.57 mm inner diameter were filled with various contrast agents, as indicated. Microfil (tube 4) is included for comparison as a standard in the field. BaSO<sub>4</sub> was prepared in normal saline using commercially supplied powder (“BaSO<sub>4</sub> Commercial”), or with an in-lab preparation (“BaSO<sub>4</sub> Precipitation”) from precipitating BaSO<sub>4</sub> from the slow mixture of BaCl<sub>2</sub> and MgSO<sub>4</sub> (replacement reaction). BaCl<sub>2</sub> (10 and 35% w/v) were mixed together with gelatin (10% w/v). (b) Magnified views of the commercial and in-lab precipitate highlight the difference in the uniformity of the BaSO<sub>4</sub> particle sizes. The scale bar is 200 microns. (c) Relative X-ray attenuation is plotted for each of the samples in A. The single plane micro CT image intensity was first inverted and then plotted as the mean intensity value (0–255 range of 8 bit image). By inverting the image intensity, increased attenuation is reflected in the positive direction. Together, these data demonstrated the smaller and more uniform particle size of the precipitated BaSO<sub>4</sub>. These data also showed comparable or improved X-ray contrast of the barium-based preparations compared with Microfil

Clearing was performed by incubating the sections in progressively increasing concentrations of glycerol (50, 75, and 85% in dH<sub>2</sub>O) for 24 hr intervals and finally in 100% glycerol for 48 hr. Z-stack bright-field images were collected and processed with the EDOF algorithm. In one instance (Figure S3), brain sections were additionally examined by inverted microscope (Leica DMI8 & DFC9000 GT camera).

### 3 | RESULTS

#### 3.1 | Comparison of barium-based X-ray contrast agents with Microfil MV-122

Barium is often exploited in CT imaging for its high X-ray attenuation (Lusic & Grinstaff, 2013). Here we explored the suitability of two barium formulations for cerebrovascular imaging by micro CT. We initially compared X-ray attenuation of the experimental materials in polyethylene (PE) tubing as a surrogate for the vasculature (i.e., “phantoms”). The PE tubing had an inner diameter of approximately 570 μm. Yellow Microfil (MV-122), a low viscosity silicone rubber resin that is radiopaque due to the inclusion of lead particles, was used as our baseline for comparison given its wide use and characterization in the field. Figure 1 shows phantoms prepared from Microfil MV-122,

BaSO<sub>4</sub> suspensions, and BaCl<sub>2</sub> in gelatin, as well as relevant controls. X-ray attenuation is reflected as the mean intensity of the image; note that the image intensity was inverted in ImageJ to reflect attenuation as a positive signal. Microfil demonstrated uniform attenuation compared with the empty PE tubing sample (Air). The BaSO<sub>4</sub> suspension prepared from a commercially obtained powder (“BaSO<sub>4</sub> Commercial”) demonstrated higher attenuation compared with Microfil, but showed significant variation in particle size. The BaSO<sub>4</sub> suspension produced by the in-lab precipitation method (“BaSO<sub>4</sub> Precipitation”) demonstrated attenuation nearly identical to the Microfil sample, but with smaller and more uniform particle size compared with the commercial BaSO<sub>4</sub>. The solution of 10% BaCl<sub>2</sub> in gelatin showed slightly lower attenuation compared with Microfil, whereas the 35% BaCl<sub>2</sub> preparation demonstrated approximately 25% greater attenuation.

#### 3.2 | Evaluation of BaCl<sub>2</sub> in gelatin as a vascular casting solution

Based on the high X-ray attenuation of the BaCl<sub>2</sub> solutions, we performed pilot studies with various concentrations of both BaCl<sub>2</sub> and gelatin to generate vascular casts of the mouse cerebral circulation (Figure 2a,b). The rationale for the gelatin preparations was to be



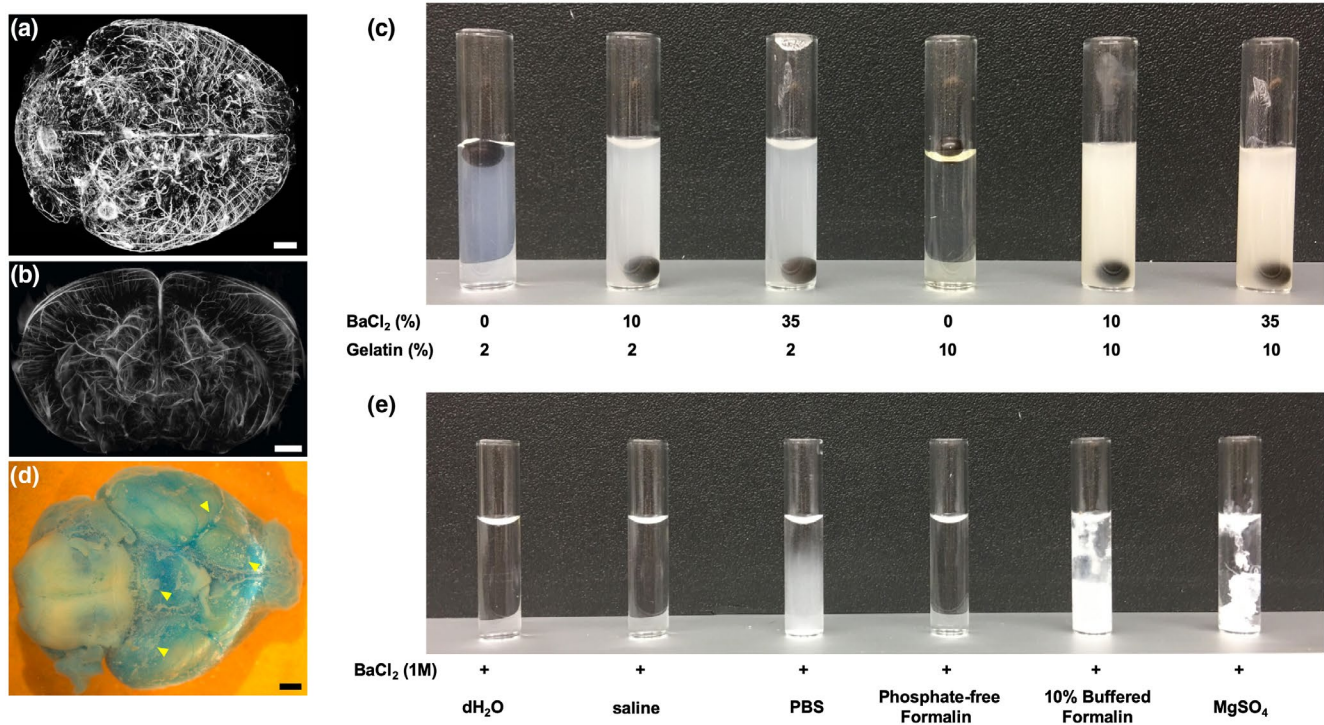


**FIGURE 2** BaCl<sub>2</sub> prevents gelatin from solidifying. (a) Representative dorsal view of micro CT 3D reconstruction following aortic perfusion with 50% BaCl<sub>2</sub>/10% gelatin of an adult mouse brain. (b) Coronal section from the above brain. Note the fuzzy contrast and low signal in surrounding tissues in the maximum intensity projection in panel A. (c) Gelatin/BaCl<sub>2</sub> mixtures were prepared and placed in 4°C for 2 hr to allow gel formation. A steel ball was placed on the top of the mixture to assess gel consistency. In gelatin solutions containing 10% or 35% BaCl<sub>2</sub>, the ball sank immediately to the bottom of the vial. These findings highlight a problem with the BaCl<sub>2</sub>/gelatin preparation—that it does not harden. The lack of hardening makes the substance difficult to contain within the vasculature and allows for Ba<sup>2+</sup> ions to more easily leach out of the vascular compartment. We observed more diffuse images with brains that were imaged after longer holding times (data not shown). (d) Ventral view of a brain following perfusion with PBS and phosphate-buffered formalin prior to BaCl<sub>2</sub> perfusion (the blue color comes from trace amounts of blue ink that were mixed in to assess perfusion). Fifty microliters of BaCl<sub>2</sub> (1 M) was added to 700 µl solutions of dH<sub>2</sub>O, saline, PBS, Shandon Formal-Fix, Fisher buffered formalin phosphate, and MgSO<sub>4</sub> (1 M in H<sub>2</sub>O). Note the extreme precipitate (yellow arrows) formed on the tissue following submersion into PBS-buffered fixative. Scale bar is 1 mm

able to perform initial infusion with a low viscosity liquid that would subsequently solidify and remain in the vasculature upon cooling. Unexpectedly, our results showed highly variable results in vascular filling and also suggested that the Ba<sup>2+</sup> was slowly diffusing from the vasculature into the surrounding brain parenchymal tissue, leading to decreased signal within the vessels and reduced contrast. Upon further evaluation, we identified two issues that compounded these problems. First, we found that BaCl<sub>2</sub> prevented gelatin from solidifying. Figure 2c demonstrates the effect of low and high BaCl<sub>2</sub> concentrations (10% and 35%, respectively) on gelatin hardening. The BaCl<sub>2</sub>/gelatin solutions (2% and 10%) were cooled at 4°C for 2 hr before a small steel ball was placed on the surface. Note that 2% or 10% gelatin alone solidified and prevented the ball from descending to the bottom of the tube. However, the steel ball sank immediately in all gelatin solutions containing BaCl<sub>2</sub>, even the solutions containing 10% gelatin. We presume that this inability of the gelatin to solidify contributed to the free diffusion of Ba<sup>2+</sup> ions within the tissue. Second, we found that the BaCl<sub>2</sub>/gelatin solution was vulnerable to forming white precipitates during infusion. These precipitates could often be seen within the surface vessels of the removed brain and likely prevented

deeper filling (Figure 2d). To determine the possible sources of barium precipitates in our protocol, we added 50 µl of 1 M BaCl<sub>2</sub> to different solutions used in our perfusion procedure (Figure 2e). Note that no precipitation occurred with the addition of BaCl<sub>2</sub> to water or saline (both of which lack phosphate groups). However, addition of BaCl<sub>2</sub> to PBS produced a cloudy white precipitate, presumably Ba<sub>3</sub>(PO<sub>4</sub>)<sub>2</sub>. It turned out that the composition of the fixative that was perfused prior to the delivery of the contrast agent was also critical. When BaCl<sub>2</sub> was added to 10% phosphate-buffered formalin, a significant precipitation resulted. In contrast, addition of BaCl<sub>2</sub> to a phosphate-free formalin solution did not produce discernable precipitate. Similar results were obtained when BaCl<sub>2</sub> was mixed with paraformaldehyde solutions prepared by diluting the 16% aqueous solution in either PBS (precipitation) or saline (no precipitation) (data not shown). As a positive control, BaCl<sub>2</sub> was added to MgSO<sub>4</sub> to produce the precipitation of BaSO<sub>4</sub>. From these results, it appears that effective infusion of BaCl<sub>2</sub> solutions into the vasculature requires that previously perfused solutions lack Ba<sup>2+</sup>-reactive compounds, such as phosphates and sulfates. Based on our findings, we determined that BaCl<sub>2</sub>/gelatin perfusion could produce robust filling of the cerebral vasculature if the mouse

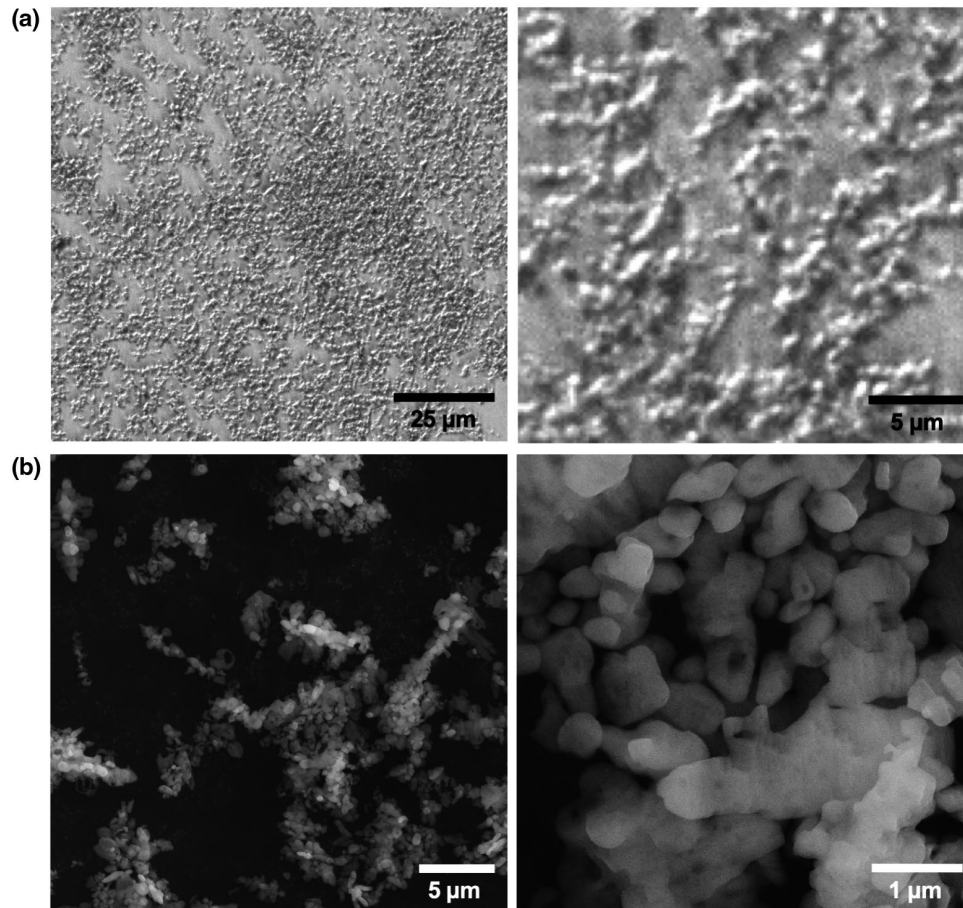


**FIGURE 3** Characterization of  $\text{BaSO}_4$  microparticles by light microscopy and scanning electron microscopy (SEM). (a) A droplet containing  $\text{BaSO}_4$  microparticles in saline was placed on a slide and coverslipped for phase contrast imaging (10X objective). Imaging shows particles of uniform size, with a tendency to form loose aggregates. (b) A droplet of  $\text{BaSO}_4$  microparticles in  $\text{dH}_2\text{O}$  was placed on a SEM specimen mount, air dried, and imaged. The drying procedure led to exaggerated aggregation of the particles. SEM analysis demonstrated single particles of 0.4 to 1.0 microns (25 to 75 percentile range)

was previously perfused with saline and phosphate-free fixatives (i.e., when PBS or phosphate-buffered fixatives were omitted) (Figure 2a,b). However, while these modifications solve the problem with variable perfusion, they do not address the issue of  $\text{Ba}^{2+}$  diffusing from the unset gelatin into underlying tissue. For this reason, we focused our subsequent attention on optimizing the infusion of  $\text{BaSO}_4$  microparticle suspensions.

### 3.3 | Preparation and analysis of $\text{BaSO}_4$ microparticle solution

From our phantom studies (Figure 1) and earlier attempts with preparing  $\text{BaSO}_4$  suspensions from commercial sources, it was clear that the large particle size contributed to the poor depth of filling. We therefore generated  $\text{BaSO}_4$  in the laboratory by a replacement reaction between  $\text{BaCl}_2$  and  $\text{MgSO}_4$  ( $\text{BaCl}_2$  [aq] +  $\text{MgSO}_4$  [aq]  $\rightarrow$   $\text{BaSO}_4$  [s] +  $\text{MgCl}_2$  [aq]).  $\text{BaCl}_2$  (0.25 M in  $\text{dH}_2\text{O}$ ) was slowly introduced (0.3 ml/min) into a rapidly stirring  $\text{MgSO}_4$  solution (0.25 M in  $\text{dH}_2\text{O}$ ), resulting in the immediate production of a fine  $\text{BaSO}_4$  precipitate ( $\text{BaSO}_4$  microparticles). These microparticles were then washed several times in normal

saline and filtered through a 40 micron basket filter prior to infusion. Examination of the resulting material by phase contrast microscopy revealed a relatively uniform population of oblong particles of  $<2$  microns that demonstrated a tendency to form loosely associated aggregates (Figure 3a) that appeared to be due to the polar nature of the  $\text{BaSO}_4$  particles (Figure S4). To further characterize the  $\text{BaSO}_4$  particles, we used scanning electron microscopy (SEM) to examine an air-dried sample (Figure 3b). SEM images demonstrated a median particle size of 0.60 microns (0.40–0.97 microns [25th to 75th percentile]) with an occasional larger particle of 2–4 microns. Therefore, to estimate the “functional size” of the microparticles in suspension, we evaluated their ability to pass through various sized filters. The microparticles passed through a 30 micron pre-separation filter (Miltenyi Biotec, 130-041-407) with no retained particles (data not shown). When the microparticles were applied to a 20 micron nylon mesh (NY20; Millipore), the majority of particles passed easily through the filter, with a small fraction retained on the filter surface. Overall, these experiments indicate that, while the individual  $\text{BaSO}_4$  microparticles are comprised of  $<1$  micron particles, in aqueous suspension, they effectively function as aggregates in the  $\leq 20$  micron range.



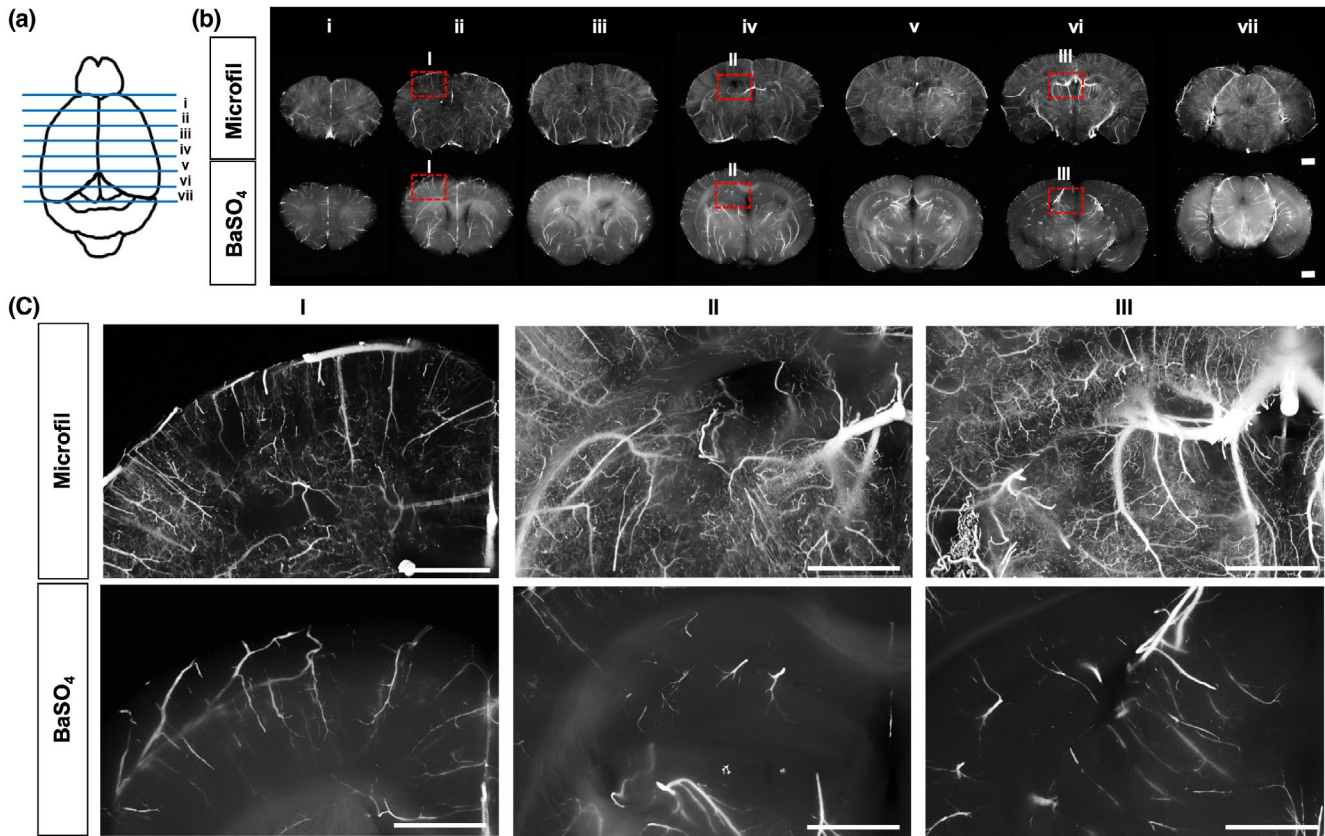


**FIGURE 4** Comparison of BaSO<sub>4</sub> microparticle and Microfil filling in optically cleared brain sections. (a) Schematic showing the approximate plane of the coronal brain sections examined by stereomicroscopy. (b) Rostral to caudal comparison of coronal sections (1 mm thickness) through the mouse brain following either aortic perfusion with Microfil (top) or BaSO<sub>4</sub> microparticle (bottom). Sections were optically cleared in glycerol before imaging. Red boxed in areas in ii, iv, and vi are magnified below in (c). Magnified views clearly depict the arterial and venous filling of penetrating arterioles and venules following Microfil perfusion versus the restriction to arteries and arterioles with BaSO<sub>4</sub> perfusion. Scale bar is 1 mm

### 3.4 | Comparison of BaSO<sub>4</sub> microparticle and Microfil vascular filling by stereomicroscopy

We next compared the distribution of infused BaSO<sub>4</sub> microparticles to Microfil compound in the adult murine brain after aortic cannulation and retrograde perfusion. Figure 4 shows both formulations in serial brain sections after clearing with glycerol and imaging by stereomicroscopy. Both preparations resulted in uniform filling throughout the brain. However, one notable difference was that the BaSO<sub>4</sub> microparticles were restricted to the arterial circulation whereas Microfil crossed the capillaries and filled the venous circulation. Figure S3 shows a BaSO<sub>4</sub> microparticle perfused brain with clear absence of BaSO<sub>4</sub> in the venules (blue arrows) despite uniform filling of penetrating arterioles (red arrows) and smaller branches <10 μm in diameter.

### 3.5 | Comparison of BaSO<sub>4</sub> microparticle and Microfil by micro CT

Once we established a method for preparing and infusing BaSO<sub>4</sub> microparticles, we compared the BaSO<sub>4</sub> and Microfil for

performing 3D vascular reconstructions by micro CT. Figure 5 shows renderings of the brain vasculature following Microfil and BaSO<sub>4</sub> microparticle perfusion. Note that the Microfil vascular cast appears more complex due to the additional filling of the venous vasculature. Consistent with the stereomicroscopy findings, the BaSO<sub>4</sub> microparticles generated an “arterial only” vascular reconstruction.

### 3.6 | Application of BaSO<sub>4</sub> microparticle and Microfil to demonstrate vascular occlusion with experimental stroke model

To compare the ability of vascular casting agents to identify occluded vascular territories, we perfused mice with Microfil or BaSO<sub>4</sub> microparticles following experimental occlusion of the MCA. A silicone-coated monofilament was introduced via the carotid artery into the CoW, where it blocked arterial flow at the origin of the MCA. This occlusion model, which is widely used in stroke research, promotes a decrease of 75% (or greater) in blood flow in the MCA territory and results in subsequent brain infarct (Fasipe et al., 2018; Liu & McCullough, 2014). Figure 6



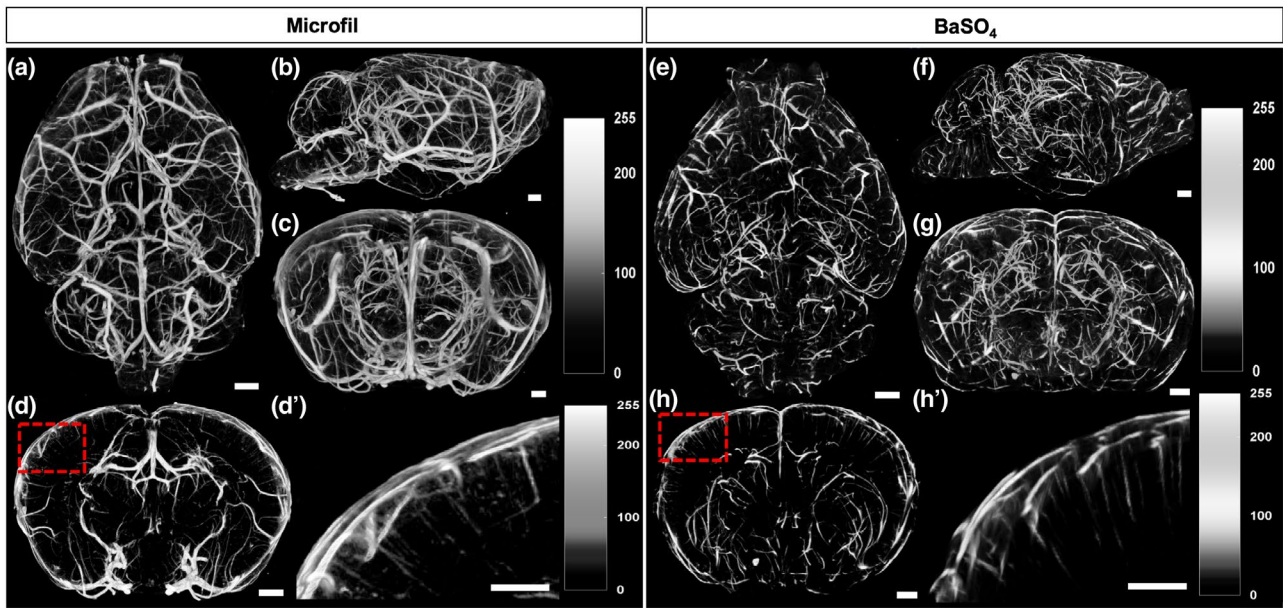


**FIGURE 5** Comparison of Microfil and BaSO<sub>4</sub> contrast agents in the adult mouse brain after retrograde aortic perfusion. Micro CT reconstructions demonstrate that Microfil (a–d') fills arterial and venous vessels whereas BaSO<sub>4</sub> (e–h') fills exclusively arterial vessels. (a,e) Dorsal views of the mouse adult brain (rostral/olfactory bulb to the top, caudal/cerebellum to the bottom). (b,f) Lateral or sagittal views (caudal to left and rostral to right) of the brain. (c,g) Coronal views (dorsal surface top, ventral surface bottom) of the brain. (d,h) Coronal reconstructions limited to 1 mm of planes taken at the level between the hippocampus and striatum through the brain. (d',h') Demonstration of smallest resolvable vessels with each contrast agent, enlarged from the red boxed in area in d and h, respectively. Data representative of  $n = 3$  per group. Scale bar is 1mm

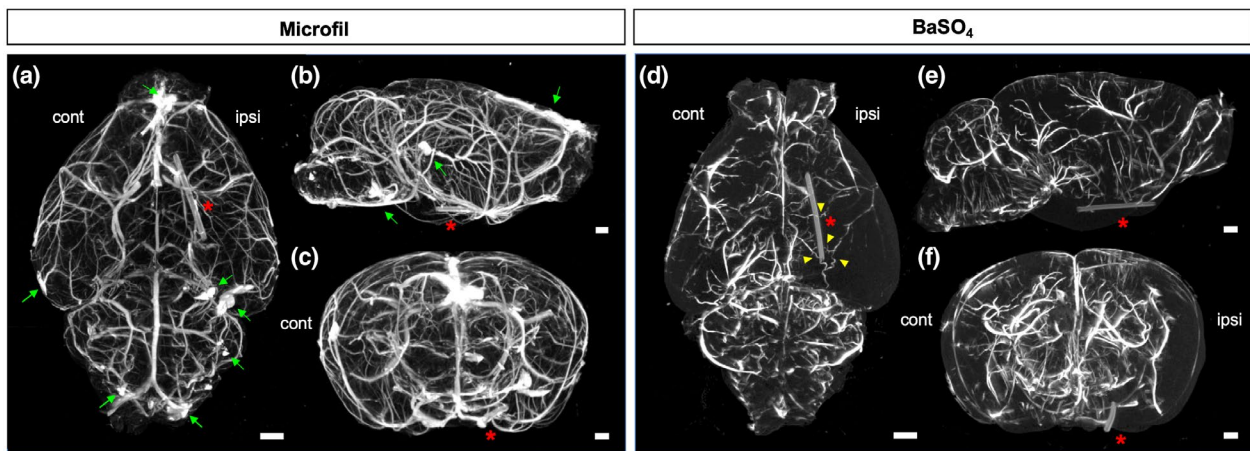


**FIGURE 6** Comparison of Microfil and BaSO<sub>4</sub> labeling of the cerebrovasculature via retrograde aortic cannulation in a murine model of cerebral stroke. (a–c) Micro CT reconstruction of Microfil perfused brains. (a) Dorsal, (b) sagittal, and (c) coronal views. (d–f) Micro CT reconstruction of BaSO<sub>4</sub> perfused brains. (d) dorsal, (e) sagittal, and (f) coronal views. The silicone occluder (\*) used for the MCAO stroke model is evident in the circle of Willis. Images are presented with the right hemisphere to the reader's right. The region ipsilateral (ipsi) or contralateral (cont) to the occlusion are indicated. Blebs or ruptures are evident throughout the brain following Microfil perfusion (green arrows), but not detected in BaSO<sub>4</sub> perfused brains. Leptomeningeal collaterals are evident connecting the middle cerebral artery (MCA) territory with the anterior and posterior cerebral artery (ACA and PCA) territories (yellow arrow heads) in the BaSO<sub>4</sub> perfused brains. The BaSO<sub>4</sub> contrast agent provides a “cleaner” view of the perfused territory due to the restriction of material to the arterial circulation. In addition, the more physiological perfusion pressure with BaSO<sub>4</sub>-based filling allows for a better match between vessel filling and tissue perfusion. Data representative of  $n = 2$  per group. Scale bar is 1 mm

shows a comparison of the Microfil and BaSO<sub>4</sub> microparticle infusions with the monofilament in place. The hemispheres ipsilateral (ipsi) and contralateral (cont) to the stroke are indicated. The

Microfil-perfused brain showed significant filling in the ipsilateral MCA territory, despite the presence of the occluder in the CoW. Several vascular bulges or possible ruptures were also evident in

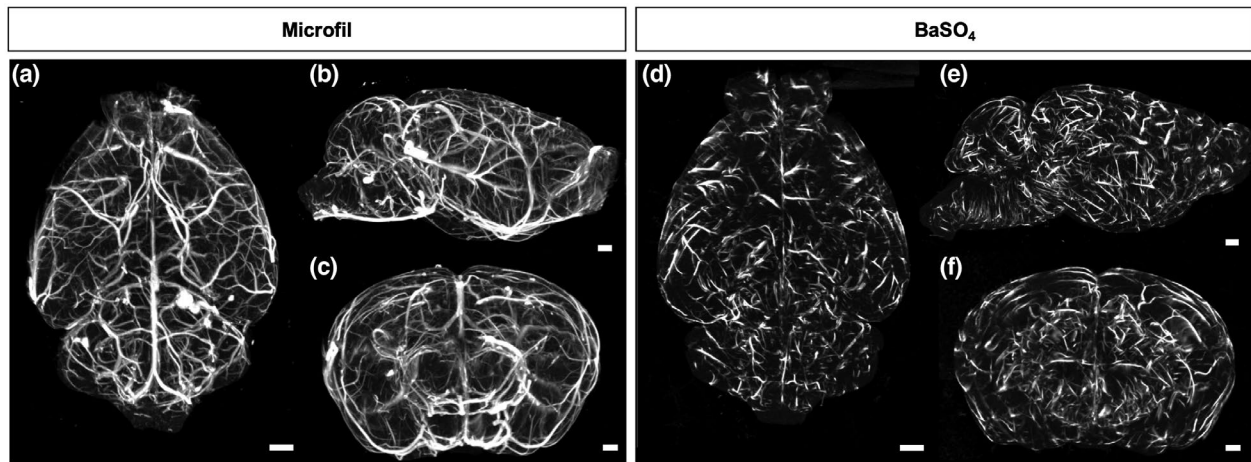


**FIGURE 7** Demonstration of transcatheter perfusion with Microfil and BaSO<sub>4</sub>. Transcatheter perfusion is easier and faster than retrograde perfusion via the thoracic aorta. However, this method can be less consistent than aortic cannulation for high-pressure applications due to leak around the cardiac puncture, breach of cardiac valves, puncture of septum, etc. Here we show representative micro CT reconstructions with both contrast agents showing the potential for similar performance to the aortic filling method. Data representative of  $n = 3$  per group. Scale bar is 1 mm

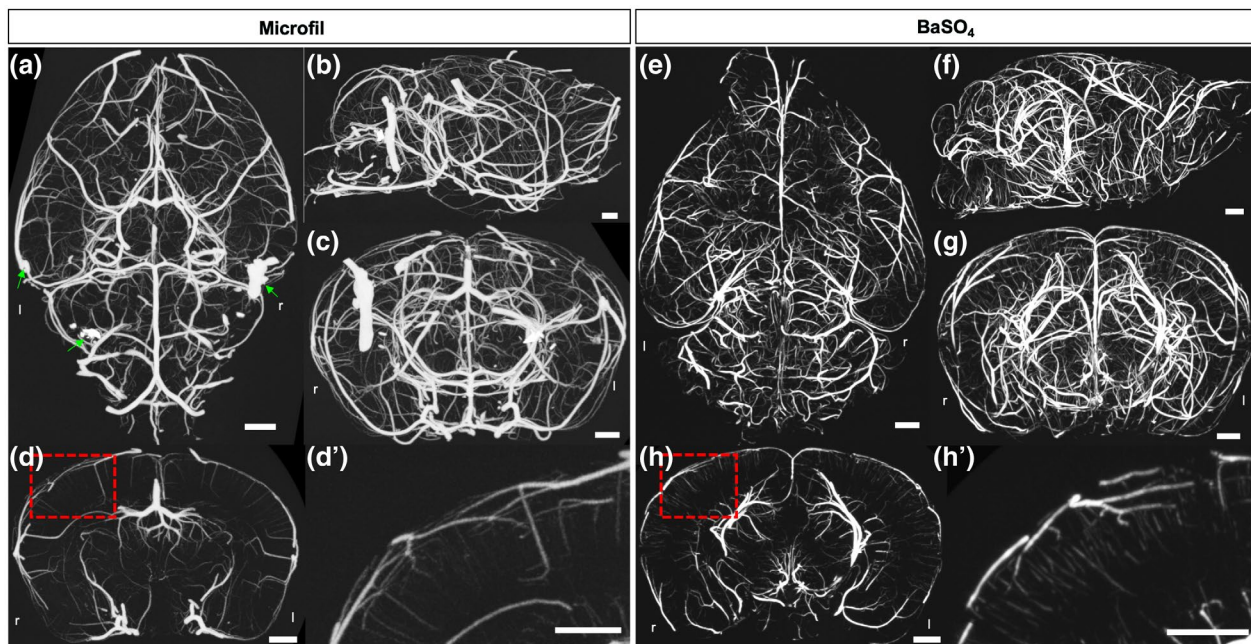


**FIGURE 8** Improved resolution of long micro CT scans by embedding in agarose. Micro CT reconstructions are presented for Microfil (a–d') and BaSO<sub>4</sub> (e–h') microparticle as in Figure 4. Maximum intensity projections from a dorsal, anterior/olfactory bulb to the top of the figure (a and e), sagittal (b and f), and coronal (c and g) view are shown, as are segmented volume renderings of a coronal view (d and h) and magnified views (d' and h'). Prior to scanning, brains were embedded in low melt agarose and sealed in a plastic screw cap vial. Imaging was performed of the brains in the tube. Sealing the samples in the tube prevented sample dehydration during the scan and eliminated the damage to the surface vessels from wrapping/unwrapping with Saran Wrap. The resulting 3D reconstructions show improved small vessel detail and lack the feathering (or shadows) seen in Figures 4–6. Green arrows denote vascular bulges and anomalies induced by high-pressure perfusion of Microfil. l = left side, r = right side for orientation. Data representative of  $n = 1$  and 2 for Microfil and BaSO<sub>4</sub> groups, respectively. Scale bar is 1 mm

the 3D reconstruction. These defects likely result from the increased pressure required to uniformly fill the vasculature when using Microfil compound. The higher pressure may also contribute to significant filling of the ipsilateral MCA territory by increased flow around the occluder or by collateral routes. In contrast, the

BaSO<sub>4</sub> microparticle-infused brain showed significantly reduced filling within the ipsilateral MCA territory and no evidence of vascular bulges or rupture. Note the clear filling of multiple collateral arterioles (yellow arrow heads) that led to partial retrograde filling of the ipsilateral MCA (Figure 6d).



### 3.7 | Evaluation of transcatheter perfusion

Retrograde perfusion by cannulation of the abdominal aorta allows for consistent and reliable perfusion of the cerebrovasculature; however, this technique requires greater surgical skill and equipment to place the catheter and is more time consuming than some simpler methods. In order to determine whether a less involved procedure could achieve similarly robust filling of the cerebral vasculature for micro CT imaging, we employed the high-throughput method of transcatheter perfusion (Figure 7). The transcatheter approach was capable of producing micro CT imaging results similar to those obtained with the more time-consuming aortic cannulation for both the Microfil compound and the BaSO<sub>4</sub> precipitate. However, the preparation was prone to leak around the needle injection site, particularly at the higher perfusion pressures. As a result, the overall rate of success with transcatheter perfusion was more variable than with aortic cannulation.

### 3.8 | Optimization of tissue preparation for micro CT imaging

Micro CT imaging of the entire murine brain required approximately 3 hr for the resolution used in this study. During this relatively long scan time, the brains are susceptible to dehydration, which results in sample shrinkage and imaging artifacts. To mitigate this problem, we loosely wrapped the brains with Saran Wrap. Nevertheless, some dehydration did occur and is evident in the higher magnifications as a feathering (or shadowing) of the images (Figure 5). Wrapping and unwrapping the exposed brain also damaged the surface vessels. As an alternative approach, we embedded the brains in low melt agarose and sealed them in a 5 ml plastic sample container prior to imaging (Figure S5). Despite the slight additional X-ray attenuation from the agarose and plastic tube, there was significantly improved resolution with this method (Figure 8, Supplemental Movies S2–S5). In addition, because the embedded brain samples do not need to be removed from the vial for imaging, the brains could be shipped by courier across the country, imaged on multiple occasions, and stored without damage to the preparation, or subsequently used for vibratome sectioning.

### 3.9 | Comparison of vascular rupture between BaSO<sub>4</sub> microparticle and Microfil

All brains were evaluated for evidence of vascular rupture, seen as blebbing in the micro CT reconstructions or the stereomicroscopy examinations. No evidence of vascular rupture was seen in the BaSO<sub>4</sub> microparticle perfused brains (0/9 brains), including after MCAO ( $n = 2$ ). In contrast, Microfil brains showed frequent evidence of vascular damage (Figure S6). Small or large ruptures were evident in 11 of the 13 Microfil perfused brains, including both MCAO brains.

## 4 | DISCUSSION

Herein, we present two barium-based micro CT contrast agents that can be easily prepared in the laboratory and offer distinct properties

compared with commercially available products, such as Microfil. Our primary reasons for exploring new vascular casting agents are (a) the need for low viscosity infusion compounds that do not perturb fragile vascular networks, (b) the desire to easily limit contrast agent to the arterial vasculature, and (c) a non-toxic, readily available alternative to lead-based Microfil.

Gelatin solutions have the desired properties of being relatively low viscosity and maintaining a workable liquid state at room temperature. Combining gelatin with a water-soluble composition of barium (BaCl<sub>2</sub>) should in principle add X-ray contrast to gelatin without contributing insoluble particles that impede vessel filling. However, our results demonstrated that preparations containing BaCl<sub>2</sub> demands excluding solutions and buffers that contain free sulfate or phosphate groups to avoid rampant particle precipitation. The process of initially perfusing the mouse with two commonly used reagents (PBS or phosphate-buffered formalin) produced a reactive environment for the BaCl<sub>2</sub> solution, which upon mixing, resulted in formation of insoluble Ba<sub>3</sub>(PO<sub>4</sub>)<sub>2</sub> within the vasculature. This in situ formation of an occlusive precipitate prevented further delivery of the BaCl<sub>2</sub> solution to downstream vasculature and thus resulted in poor visualization of the microvasculature. Our solution to this issue was to perfuse the mouse initially with saline and then phosphate-free fixative (either commercially prepared product or mixture of PFA in saline).

Even though we were able to modify our protocol to consistently deliver BaCl<sub>2</sub>/gelatin, the contrast diffused within the tissue leading to less crisp images upon 3D reconstruction. We speculate that the free Ba<sup>2+</sup> ions were able to migrate more quickly from the non-setting gelatin mixture. Because of this characteristic, samples had to be scanned soon after infusion. If processing multiple samples, the requirement for prompt scanning presents a significant rate limiting factor (with each high-resolution brain scan requiring approximately 3, or more, hours to complete). To address the failure of gelatin solutions to cure, we explored the use of BaCl<sub>2</sub> in conjunction with low melt agarose (Figure S7). While BaCl<sub>2</sub>/agarose solutions did cure (for 10% and 35% BaCl<sub>2</sub>), the procedure required maintaining both the solution and mouse body cavity at a warm temperature during infusion to prevent premature gelling of the contrast agent, which presents its own set of complicating factors.

Like BaCl<sub>2</sub>, BaSO<sub>4</sub> has excellent X-ray attenuation properties and is frequently used in humans for CT imaging of the gastrointestinal tract (Lusic & Grinstaff, 2013). For producing vascular casts, BaSO<sub>4</sub> can provide a good alternative to toxic lead-containing compounds, such as Microfil (Oldendorf, 1989). Somewhat surprisingly, commercial preparations of BaSO<sub>4</sub> displayed a large variation of particle sizes (see Figure 1) which contributes to poor delivery into the microvasculature. To address this variability in particle size, we generated BaSO<sub>4</sub> in the laboratory using a replacement reaction. The resulting particles appeared to be a relatively uniform size of 0.4 to 1 microns. Interestingly, the microparticles appeared to function as slightly larger particles, possibly due to the potential to loosely aggregate owing to the polar nature of the BaSO<sub>4</sub> particles (Gao et al., 2011) (and Figure

S4). We tested the functional size of the microparticles with different sized filters. BaSO<sub>4</sub> microparticles completely passed through a 30 μm pre-separation filter. With a 20 μm nylon mesh, the majority of microparticles passed, with a small residual on the membrane surface. More aggressive flushing could force the remaining particles through, which suggests that the particles may behave as a loose aggregate with a functional size of ≤20 microns. Consistent with this assessment, our perfusion studies showed visible BaSO<sub>4</sub> in large arterial microvessels and smaller arterial vessels down to approximately 10 microns in diameter. However, BaSO<sub>4</sub> was not observed in the venous vasculature (Figures S2 and S3), suggesting that the microparticles become trapped at some point between the distal arterioles and the capillaries.

BaSO<sub>4</sub> microparticles have an additional characteristic that makes them attractive for vascular casting applications, namely that fluid can still pass through the particles even after they have accumulated in the microvasculature. The capacity for solution to move through the packed particle matrix (like water in a French drain) allows flow to continue after filling the microvessels and for infusion pressure to remain low over a wide range of filling volume. As evidence of this, infusion of variable amounts of BaSO<sub>4</sub> microparticles (5 to 10 ml) failed to induce significant back pressure and no evidence of vascular bulging or rupture was observed in any of the microparticle perfused brains (0/11), unlike our results with Microfil (11/13).

In summary, we present two alternatives to polymer-based systems for performing CT-based vascular reconstructions, each with distinct advantages. BaCl<sub>2</sub>/gelatin preparations, when combined with phosphate-free perfusion and fixation reagents, are effective for low viscosity filling of the arterial and venous circulations. For best results, samples should be scanned soon after perfusion. For more long-term contrast stability or limiting contrast to the arterial circulation, BaSO<sub>4</sub> microparticles provide an inexpensive contrast agent that provides uniform filling of the arteries/arterioles with low perfusion pressure. Overall, these formulations, when combined with micro CT, offer the advantage of being able to observe cerebrovasculature in a non-transparent, intact adult mouse brain, in 3D, independent of sample thickness, shortly after tissue collection (1 day post perfusion), without the need for complicated clearing and immunohistochemical protocols or advanced confocal imaging methodologies (e.g., SPIM or light sheet microscopy) and without regard to imaging depth.

#### 4.1 | Limitations

One of the limitations of these methods is the inability to clearly resolve the capillary vasculature. With Microfil or BaCl<sub>2</sub>/gelatin infusion, the capillaries were clearly perfused with contrast agent, as the material passed from arteries to veins. The lack of visible capillaries likely reflects insufficient volume of contrast agent in these microvessels to permit enough X-ray attenuation compared to the surrounding tissue. However, depending on experimental goals, this limitation may actually help “decluster” the analysis and permit cleaner visualization of the vasculature exclusive of the capillaries. An additional limitation of the current study is that experiments were performed exclusively in a single strain of mature adult male mice. Our choice for limiting studies to this population was primarily

motivated by the need to perform initial characterization in a homogeneous cohort to limit variability due to differences in strain, age, or sex. Future studies will be required to explore possible strain-, age-, and sex-specific differences in the anatomy of the cerebral small vasculature.

## DECLARATION OF TRANSPARENCY

The authors, reviewers, and editors affirm that in accordance with the policies set by the Journal of Neuroscience Research, this manuscript presents an accurate and transparent account of the study being reported and that all critical details describing the methods and results are present.

## ACKNOWLEDGMENTS

We thank Ms. Karen Berman de Ruiz for excellent care and maintenance of our mouse colony, and Mr. Jason Kirk and Dr. Chih-Wei Hsu at the Optical and Imaging and Vital Microscopy (OIVM) (Dr. Mary Dickinson, Director) core at BCM for support with imaging and data processing. We also thank Dr. Nimesh Patel for assistance with SEM imaging in the Biological Imaging Core (Dr. Alan R. Burns, Director) at the College of Optometry, University of Houston.

## CONFLICT OF INTEREST

The authors declare no competing or financial interests.

## AUTHOR CONTRIBUTIONS

*Conceptualization*, S-H.H., A.M.H., S.P.M., and J.D.W.; *Methodology*, S-H.H., S.P.M., T.W., A.R.B., and J.D.W.; *Investigation*, S-H.H., A.M.H., J.M.S., A.N.B., T.W., A.R.B., S.P.M., and J.D.W.; *Resources*, S.P.M., A.N.B., and J.D.W.; *Writing - Original Draft*, S-H.H., S.P.M., and J.D.W.; *Writing - Review & Editing*, S-H.H., A.R.B., and A.M.H.; *Visualization*, S-H.H., A.M.H., S.P.M., and J.D.W.; *Supervision*, S.P.M. and J.D.W.; *Project Administration*, S.P.M. and J.D.W.; *Funding Acquisition*, S-H.H., A.M.H., A.R.B., S.P.M., and J.D.W.

## ORCID

Sean P. Marrelli  <https://orcid.org/0000-0001-8476-4785>

Joshua D. Wythe  <https://orcid.org/0000-0002-3225-2937>

## REFERENCES

- Clark, D. P., & Badea, C. T. (2014). Micro-CT of rodents: State-of-the-art and future perspectives. *Physica Medica*, 30(6), 619–634. <https://doi.org/10.1016/j.ejmp.2014.05.011>
- Ehling, J., Theek, B., Gremse, F., Baetke, S., Möckel, D., Maynard, J., ... Lammers, T. (2014). Micro-CT imaging of tumor angiogenesis: Quantitative measures describing micromorphology and vascularization. *American Journal of Pathology*, 184(2), 431–441. <https://doi.org/10.1016/j.ajpath.2013.10.014>



- Fasipe, T. A., Hong, S.-H., Da, Q. I., Valladolid, C., Lahey, M. T., Richards, L. M., ... Marrelli, S. P. (2018). Extracellular vimentin/VWF (von Willebrand factor) interaction contributes to VWF string formation and stroke pathology. *Stroke*, *49*(10), 2536–2540. <https://doi.org/10.1161/strokeaha.118.022888>
- Gao, W., Zhou, B., Ma, X., Liu, Y., Wang, Z., & Zhu, Y. (2011). Preparation and characterization of BaSO<sub>4</sub>/poly(ethylene terephthalate) nanocomposites. *Colloids and Surfaces A: Physicochemical and Engineering Aspects*, *385*, 181–187. <https://doi.org/10.1016/j.colsurfa.2011.06.015>
- Ghanavati, S., Yu, L. X., Lerch, J. P., & Sled, J. G. (2014). A perfusion procedure for imaging of the mouse cerebral vasculature by X-ray micro-CT. *Journal of Neuroscience Methods*, *221*, 70–77. <https://doi.org/10.1016/j.jneumeth.2013.09.002>
- Jorgensen, S. M., Demirkaya, O., & Ritman, E. L. (1998). Three-dimensional imaging of vasculature and parenchyma in intact rodent organs with X-ray micro-CT. *American Journal of Physiology*, *275*(3), H1103–H1114. <https://doi.org/10.1152/ajpheart.1998.275.3.H1103>
- Liu, F., & McCullough, L. D. (2014). The middle cerebral artery occlusion model of transient focal cerebral ischemia. *Methods in Molecular Biology*, *1135*, 81–93. [https://doi.org/10.1007/978-1-4939-0320-7\\_7](https://doi.org/10.1007/978-1-4939-0320-7_7)
- Lusic, H., & Grinstaff, M. W. (2013). X-ray-computed tomography contrast agents. *Chemical Reviews*, *113*(3), 1641–1666. <https://doi.org/10.1021/cr200358s>
- Marxen, M., Thornton, M. M., Chiarot, C. B., Klement, G., Koprivnikar, J., Sled, J. G., & Henkelman, R. M. (2004). MicroCT scanner performance and considerations for vascular specimen imaging. *Medical Physics*, *31*(2), 305–313. <https://doi.org/10.1118/1.1637971>
- Oldendorf, W. H. (1989). Trophic changes in the arteries at the base of the rat brain in response to bilateral common carotid ligation. *Journal of Neuropathology and Experimental Neurology*, *48*(5), 534–547. <https://doi.org/10.1097/00005072-198909000-00004>
- Vandeghinste, B., Trachet, B., Renard, M., Casteleyn, C., Staelens, S., Loeys, B., ... Vandenberghe, S. (2011). Replacing vascular corrosion casting by in vivo micro-CT imaging for building 3D cardiovascular models in mice. *Molecular Imaging and Biology*, *13*(1), 78–86. <https://doi.org/10.1007/s11307-010-0335-8>
- Vasquez, S. X., Gao, F., Su, F., Grijalva, V., Pope, J., Martin, B., ... Reddy, S. T. (2011). Optimization of microCT imaging and blood vessel diameter quantitation of preclinical specimen vasculature with radiopaque polymer injection medium. *PLoS One*, *6*(4), e19099. <https://doi.org/10.1371/journal.pone.0019099>

## SUPPORTING INFORMATION

Additional supporting information may be found online in the Supporting Information section at the end of the article.

**Figure S1.** Summary of BaSO<sub>4</sub> preparation procedure.

**Figure S2.** Retrograde aortic perfusion and results using Microfil and BaSO<sub>4</sub> precipitate.

**Figure S3.** BaSO<sub>4</sub> microparticles are limited to the arterial vasculature.

**Figure S4.** Disruption of BaSO<sub>4</sub> microparticle aggregation with ionic detergents.

**Figure S5.** Brains embedded in agarose for micro CT imaging.

**Figure S6.** Examples of small and large vascular ruptures with Microfil perfusion.

**Figure S7.** BaCl<sub>2</sub> does not prevent hardening of agarose.

**Movie S1.** Precipitation of BaSO<sub>4</sub> by mixing solutions of BaCl<sub>2</sub> and MgSO<sub>4</sub>.

**Movie S2.** Brain vascular casting with Microfil.

**Movie S3.** Brain vascular casting with Microfil (red/green stereo version).

**Movie S4.** Brain vascular casting with BaSO<sub>4</sub>.

**Movie S5.** Brain vascular casting with BaSO<sub>4</sub> (red/green stereo version).

Transparent Peer Review Report

Transparent Science Questionnaire for Authors

**How to cite this article:** Hong S-H, Herman AM, Stephenson JM, et al. Development of barium-based low viscosity contrast agents for micro CT vascular casting: Application to 3D visualization of the adult mouse cerebrovasculature. *J Neuro Res*. 2019;00:1–13. <https://doi.org/10.1002/jnr.24539>